

COBEM-2023- 1326

FINITE ELEMENT ANALYSIS OF THE MECHANICAL STRUCTURE OF AN HYBRID ORTHOSIS

Francielle Aparecida da Paz

Department of Mechanical Engineering, Universidade Federal de Minas Gerais – UFMG
6627, Antônio Carlos Avenue, Belo Horizonte, MG, Zip Code: 31270-901, Brazil
franciellepaz@ufmg.br

Arthur Torres Caetano

Graduate Program in Mechanical Engineering, Universidade Federal de Minas Gerais – UFMG
6627, Antônio Carlos Avenue, Belo Horizonte, MG, Zip Code: 31270-901, Brazil
arthurcaetano@ufmg.br

Matheus Carvalho Barbosa Costa

Graduate Program in Mechanical Engineering, Universidade Federal de Minas Gerais – UFMG
6627, Antônio Carlos Avenue, Belo Horizonte, MG, Zip Code: 31270-901, Brazil
mt94_carvalho@hotmail.com

João Paulo Fernandes Bonfim

Graduate Program in Electrical Engineering, Universidade Federal de Minas Gerais – UFMG
6627, Antônio Carlos Avenue, Belo Horizonte, MG, Zip Code: 31270-901, Brazil
jpfb2015@ufmg.br

Guilherme de Paula Rúbio

Graduate Program in Mechanical Engineering, Universidade Federal de Minas Gerais – UFMG
6627, Antônio Carlos Avenue, Belo Horizonte, MG, Zip Code: 31270-901, Brazil
guilhermerubio@ufmg.br

Fernanda Márcia Rodrigues Martins Ferreira

Graduate Program in Mechanical Engineering, Universidade Federal de Minas Gerais – UFMG
6627, Antônio Carlos Avenue, Belo Horizonte, MG, Zip Code: 31270-901, Brazil.
University of Montpellier, CAMIN, INRIA
860, Rue Saint Priest, Zip Code: 34095, France.
fernandaferreira.to@gmail.com

Lucas Oliveira da Fonseca

University of Montpellier, CAMIN, INRIA, France.
860, Rue Saint Priest, Zip Code: 34095, France.
lucas.fonseca@inria.fr

Henrique Resende Martins

Graduate Program in Electrical Engineering, Universidade Federal de Minas Gerais – UFMG
6627, Antônio Carlos Avenue, Belo Horizonte, MG, Zip Code: 31270-901, Brazil.
henriquerm@gmail.com

Claysson Santos Bruno Vimieiro

Graduate Program in Mechanical Engineering, Universidade Federal de Minas Gerais – UFMG
6627, Antônio Carlos Avenue, Belo Horizonte, MG, Zip Code: 31270-901, Brazil.
Graduate Program in Mechanical Engineering, Pontifícia Universidade Católica de Minas Gerais – PUC Minas
500, Dom José Gaspar Avenue, Belo Horizonte, MG, Zip Code: 30535.901, Brazil.
claysson@gmail.com

Abstract. *The most common sequelae caused by stroke are motor limitations in the upper limbs, which hinder the affected individual from performing daily activities independently. To alleviate these consequences, a hybrid orthosis that combines mechanical structures and Functional Electrical Stimulation (FES) can be used in the rehabilitation of these individuals. This study aims to evaluate structurally the orthosis using Finite Element Analysis based on biomechanical data. The torque curve at the elbow joint was obtained using OpenSim software, simulating the flexion movement of the arm with an additional 1 kg mass on the hand. A maximum torque of 7 Nm occurring at 90° was obtained, and this value was used in the simulated model in Ansys Mechanical. The maximum resulting stress was observed in the screw receiving the impact of the movement with a value of 120.38 MPa and the corresponding strain of 0.36%. With this geometry, it was obtained a functional and safe orthosis for the users.*

Keywords: *Hybrid orthosis, Biomechanics, Functional Electrical Stimulation, Finite Element Analysis, OpenSim.*

1. INTRODUCTION

According to the World Health Organization (WHO, 2021), stroke is the second most common cause of death worldwide, resulting in chronic disabilities in over 50% of survivors due to brain tissue damage (Donkor, 2018). Among individuals with stroke sequelae, there is a significant group that has upper limb movement limitations, which affects their ability to perform simple daily activities (Lawrence et al., 2001). In this context, robotic rehabilitations have been developed as alternatives to assist in the recovery of these individuals, enabling them to regain independence in performing daily activities. This type of therapy allows for greater individualization of treatment than conventional approaches, as it allows for better control over the number and intensity of repetitions performed, thereby increasing the effectiveness of rehabilitation (Ferreira et al., 2022).

In robotic rehabilitation applications, active orthoses with mechanical actuators to generate limb movement or semi-active orthoses that modify the mechanical characteristics of the orthosis without directly exerting mechanical work on the limb are commonly used (Ministério da Saúde, 2019).

In orthosis design for rehabilitation after stroke, the reduction of mass and volume is always desired due to the skeletal and muscular conditions of the user. Therefore, the parts of the device are manufactured using low-density materials with high mechanical strength, such as aluminum alloys and polymers. The parts are designed to be anatomically attached to the user's limbs. In the literature, various models of orthoses for robotic rehabilitation have been reported (Rubio et al., 2019; Rubio et al., 2021; Lavrenko and Lebedysnskyi, 2022). Among these, Rubio et al. (2021) developed a prototype orthosis using low-density materials with good mechanical strength. They also employed a robotic system with electric motors to rotate the user's elbow and a hand module with finger activation, using steel cables connected to electric motors. Based on this orthosis model, a hybrid structure was designed, in which the passive robotic system consisting of electric motors was replaced with Functional Electrical Stimulation (FES), aiming to reduce the orthosis mass through muscle activation.

An important step in the development of this hybrid orthosis is structural calculations, and it is necessary to estimate the forces exerted by the user's muscles, activated by FES, on this device. Variations in muscle mobility among orthosis users add complexity to the structural calculation. Thus, ensuring structural integrity, along with appropriate mobility and safety for users during clinical treatment, is essential for the success of rehabilitation. Therefore, the objective of this study was to validate the design of the new hybrid orthosis for upper limbs using Finite Element Analysis (FEA) to simulate and propose improvements in the mechanical structure based on biomechanical data collected via simulation in the OpenSim software.

2. METHODOLOGY

To validate the structure of the hybrid orthosis, several steps were necessary, starting with the 3D modeling of the orthosis using Computer-Aided Design (CAD) software. The biomechanical data of elbow flexion were obtained using OpenSim software, and the static calculation of the orthosis structure was performed using Ansys Mechanical software for structural analysis. In this section, will be presented the mathematical model, biomechanical simulations, and boundary conditions applied in the structural calculation.

2.1 Hybrid orthosis design

The orthosis was designed to be secured to the user's forearm and arm using a rigid Polyvinyl Chloride (PVC) mold wrapped in an Ethylene Vinyl Acetate (EVA) cover. In the arm, this mold is directly screwed onto the structure of a rod of the orthosis, while in the forearm, this structure is screwed onto two pieces 3D printed in Polylactic Acid (PLA), which are allocated as a sliding joint on the forearm rods. To allow elbow flexion, the orthosis was designed with a rotational joint that will be positioned on the same axis of rotation of the elbow joint for each user. As muscle-tendon flexibility influences the ability of elbow flexion and extension, which varies for each individual, the orthosis was

designed with an angular adjustment system that allows for quick modifications for each user, enabling personal adjustments with a wide angular range - 20° to 180° - respectively for flexed and fully extended elbow positions.

The materials will be applied according to the stress in each component. The rods will be made of T6006 aluminum alloy. The rotation limiter applied to the elbow and the transverse limiter for the forearm will be manufactured from PLA thermoplastic. The orthosis, developed using SolidWorks® software, is presented in Figure 1.

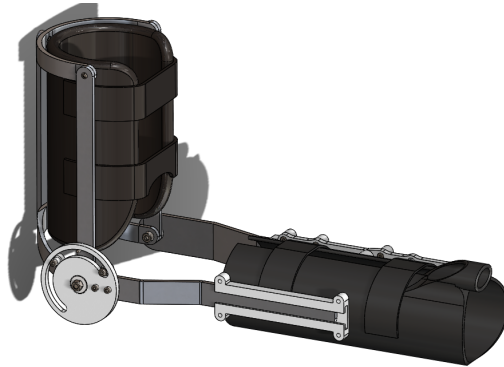


Figure 1. 3D model of the orthosis device.

2.2 Acting torque during elbow flexion

As this model will be activated via FES (Ferreira, 2022), which will contract the elbow flexor muscles, determining the forces acting on the orthosis structure becomes a complex task, as the muscular force-generating capacity varies greatly among individuals, and the muscle mass of individuals has significant variability. The values of mass and geometry parameters for the upper limbs were extracted from the study conducted by Rubio et al. (2021), with the forearm having a mass of 1.376 kg and a length of 0.264 m, the hand having a mass of 0.516 kg and a length of 0.196 m, based on proportions for an adult male with a height of 1.83 m and a weight of 85 kg. This estimate is above the expected average for a Brazilian man between 35 and 44 years old, which is the age group with the highest average weight, with an average height of 1.71 m and 74.6 kg (IBGE, 2009).

The torque values were calculated using the open-source software OpenSim, which simulates movements based on concepts from biology, neuroscience, mechanics, and robotics (Seth, 2018). The chosen model to simulate the arm flexion movement was the Arm26, which is available for open-source download on the OpenSim platform. This model is a simplification of arm anatomy using rigid bodies, bones, and six muscles, including the long head, lateral head, and medial head of the triceps, the long and short heads of the biceps, and the brachialis, which are the most involved muscles in arm flexion. The simulation is capable of mathematically reproducing dynamic activation, force-length and force-velocity relationships, and muscle-tendon dynamics (Seth, 2018).

One of OpenSim's tools used to solve the mathematical models is inverse dynamics, which, based on known kinematics, can determine the forces and torques at each joint responsible for a given movement. This result is obtained by solving the classical equation of motion Eq. (1), where q , q' , and q'' are vectors representing position, velocity, and acceleration, respectively, $M(q)$ is the mass matrix, $C(q, q')$ is the vector of Coriolis and centrifugal forces, $G(q)$ is the vector of gravitational forces, and τ is the generalized force vector (Opensim, 2023).

$$M(q)q'' + C(q, q') + G(q) = \tau \quad (1)$$

In the software environment, to find the torque curve of elbow flexion, the Inverse Dynamic tool was used with the 3D model of the upper limb with the previously described geometry and mass data, with a displacement of 29° per second, totaling 5 seconds within a range of 0 to 145°, corresponding to a full arm flexion. This process is schematically illustrated in Figure 2. During elbow flexion, the hand and fingers remained static in the anatomical position. The simulation was performed with and without the additional 1 kg mass attached to the hand, as shown in Figure 3. Finally, to validate the simulation performed in OpenSim software, the results obtained for elbow flexion without additional mass on the hand were compared with the mathematical model described in Eq. (2) found in the literature (Rubio, 2021).

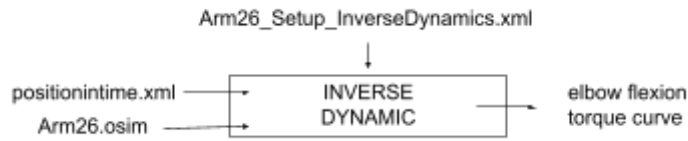


Figure 2. OpenSim diagram for Inverse Dynamics of the elbow.

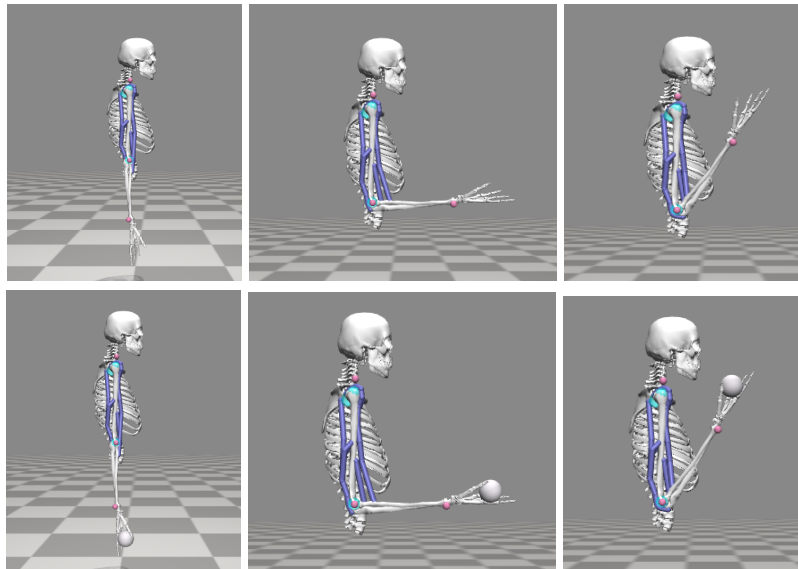


Figure 3. Musculoskeletal OpenSIM upper limb model.

$$T_0 = P \cdot R_g \cdot \sin(\Theta_0 + w \cdot \Delta t) \quad (2)$$

2.3 FEA simulation

To seek simplifications of the finite element analysis model, two structural analyses were performed using the Ansys Mechanical[®] software, one to analyze the mechanical structure of aluminum components acting together and another to validate the PLA-made limiter. The simulations were conducted on a computer running the Microsoft Windows 10[®] operating system, with 32 GB of RAM, Intel[®] Core™ i5-12500 H processor, and NVidia[®] RTX 3050™ graphics card.

2.3.1 Model and materials

In both simulations described afterwards, the model shown in Figure 4a was used. The considered mechanical properties of the applied materials are shown in Table 1, the application of the materials to each component is presented in the Figures 4b and 4c. For the PLA was assumed isotropic behavior for simulation simplification.

Table 1. Mechanical properties of the applied materials on the simulation.

Components	Material	Yield Strength (MPa)	Maximum elongation (%)
Orthosis mechanical structure ⁽¹⁾	Aluminum alloy 1100H4	95	5
Screws ⁽²⁾	Steel 30MnVS6	800	14
Limiter and bushings ⁽³⁾	PLA	54,1	1,568

⁽¹⁾Methalgata (2019), ⁽²⁾Ovako (2023), ⁽³⁾Ansys (2023).

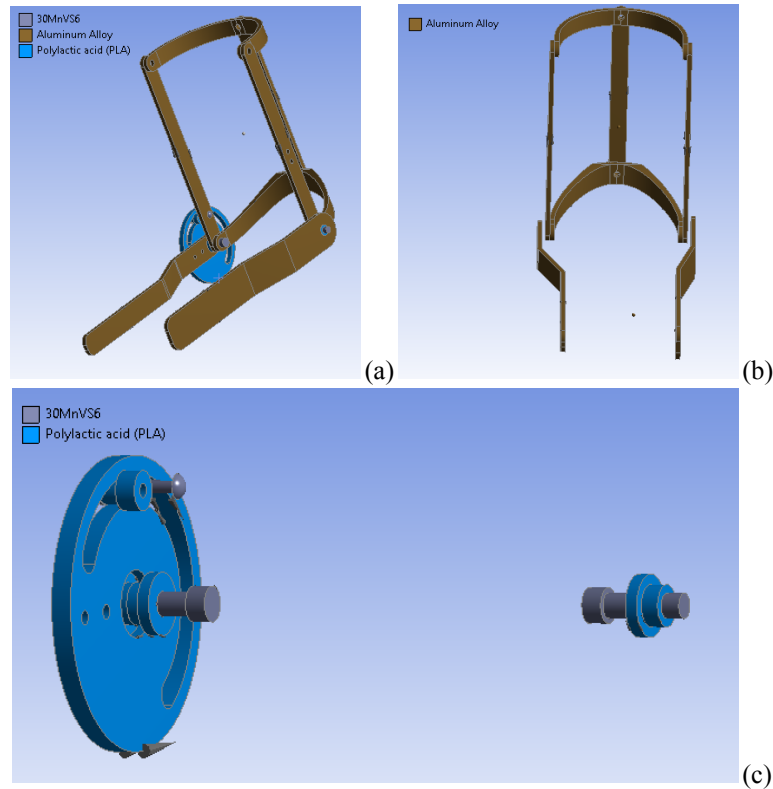


Figure 4. Materials applied on the orthosis structure for FEA: (a) Full model (b) Aluminum parts (c) Parts in 30MnVS6 steel and PLA.

2.3.2 Analysis of the aluminum mechanical structure

For structural analysis, the orthosis was positioned where the highest loading occurs during the elbow flexion movement, as determined by the simulation in OpenSim software. The masses of the forearm and the hand holding a 1 kg object were imposed on the bars that support the user's forearm, resulting in a distributed load of 2.8 kg on their inner surfaces. The maximum torque acting on the elbow was converted into a force of 31N and applied to the most extreme vertical surfaces - at a distance of 0.225 m from the orthosis joint - shown in Figure 4(a), with a direction of application consistent with the torque during elbow flexion movement. The central bar of the upper portion of the orthosis, where the user's arm is supported, was considered as a rigid element and fixed, and all the contacts among the structure components were considered as bonded. The simulation also considered the effect of gravity with a value of 9.8066 m/s^2 . The remaining boundary conditions are presented in Figure 5a, where A represents gravity, B represents the 31N force, C represents the fixed bar and D represents the distributed mass. The mesh of the model uses deformable linear elements consisting of 63,434 elements and 118,627 nodes, the vertical bars have quadrilateral elements and the others have hexahedron elements, as shown in Figure 5b.

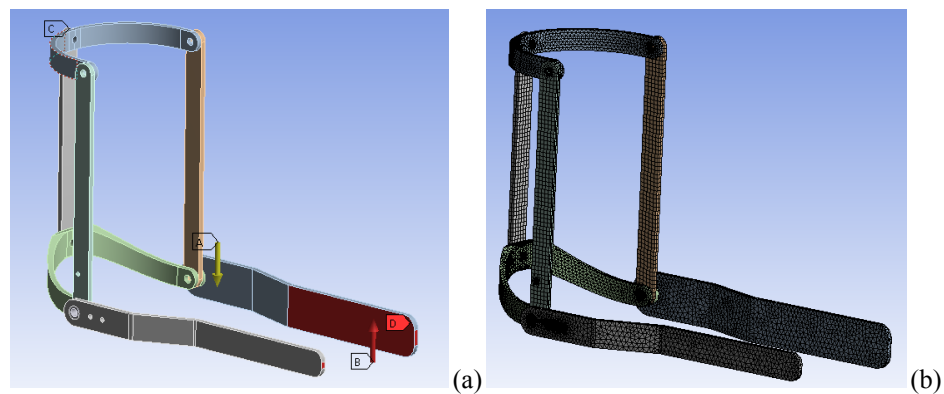


Figure 5. FEA in the orthosis aluminum structure: (a) Boundary conditions, and (b) meshed model.

2.3.3 Analysis of the PLA limiter

The same boundary conditions used in the model without the limiter were adopted. However, for the bushings, screws, and nuts belonging to the rotational joint of the orthosis, a connection that allows rotation between these mechanisms was used, enabling the rotation of the connected bars. The pin and disk were modeled as bonded contact, since the disk is attached to the bars by screws, causing them to move together. To ensure the limiter operation, the pin must be fixed to the disc in a position that stops the movement when the elbow reaches 90 degrees. The limiter was adjusted to lock the elbow flexion movement at the position of maximum torque, to verify if the component could withstand the loading, as shown in Figure 6a.

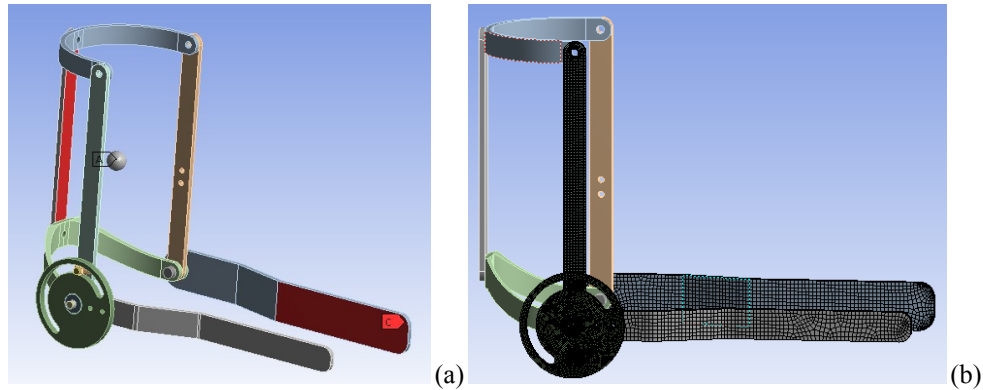
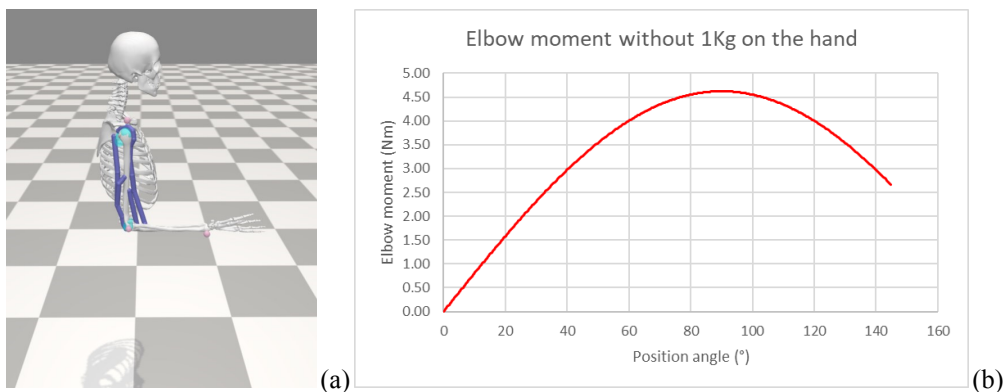


Figure 6. FEA to validate the PLA limiter: (a) Boundary conditions, and (b) meshed model.

The model was simplified, considering only the forearm bars, the screws in the rotational joint allowing elbow articulation, and the angular motion limiter, as the aluminum structure had already been validated. Therefore, the arm bars were considered rigid bodies, except for the bars connecting to the limiter. The mesh of the model was generated using deformable linear elements, consisting of 115,609 elements and 289,226 nodes, the elements in the bars and in the limiter are quadrilaterals and in the other components they are hexahedrons, as shown in Figure 6(b).

3. RESULTS AND DISCUSSION

It is possible to observe in Figure 1 that the hybrid orthosis with FES activation provides a large reduction - with a calculated mass of 1.1 kg - when compared to devices with electric motor actuation (Rubio et al., 2021). The torque curves in Figure 7 show the relationship between the elbow torque and the elbow flexion angle, with some positions illustrated in Figures 7a and 7c. The graph shows the expected behavior by Eq. (2), and also the minimum torques occur when the elbow is fully extended. On the other hand, the maximum torques of 4.62 Nm, without added mass to the hand, and 7 Nm, with added mass of 1kg to the hand, both occur at a 90° angle, that is, when the forearm is perpendicular to the arm, Figure 7b and 7d respectively. The maximum torque value without mass addition is in agreement with a previous study (Rubio, 2021) which obtained a maximum torque of 4.8 Nm, in comparison, this study presents a difference of 3.75% from the data existing in literature, that was calculated using the mathematical model described in Eq. (2).



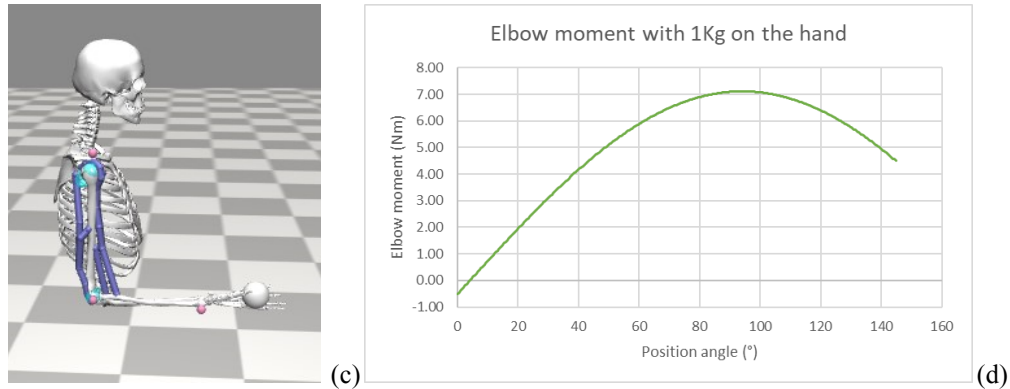


Figure 7. OpenSim simulations with the respective torque curve: (a) Elbow flexion without added mass (b) Torque (c) Elbow flexion with added mass (d) Torque x Angle.

The static simulations of the orthosis structure were performed by applying a load of 31 N, equivalent to the maximum torque of 7 Nm obtained in OpenSim software, at the end of the rods - 0.225 m from the orthosis joints - that orthosis joint that supports the forearm. In addition, the weight of the limbs was inserted as described in Section 2.2. Figure 8a shows that the maximum von Mises stress for the defined boundary conditions is 22.64 MPa and occurs in the contact region between the upper curved rod and the vertical rod, and the minimum stress is 0.05 Pa, and occurs on the fixed bar, however on the lateral surface, Figure 8a. The maximum equivalent elastic deformation is 0.19% and occurs in the left bushing between the horizontal and vertical rods, while the minimum of approximately 0% occurs on the fixed surface, Figure 8b.

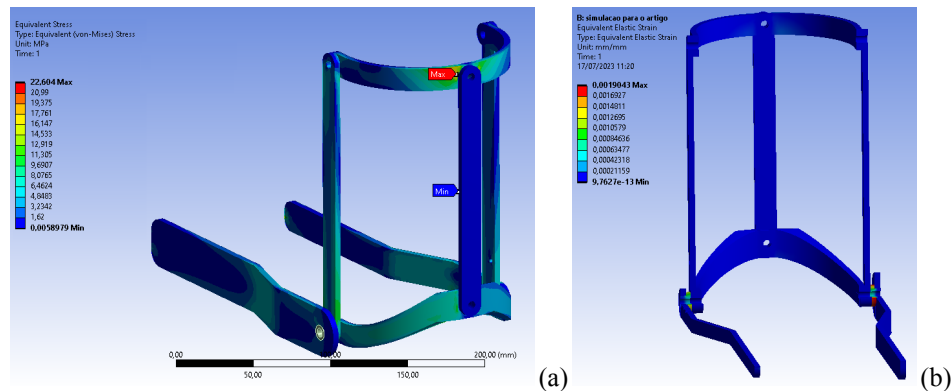


Figure 8. Metal structure simulation results: (a) von Mises stress distribution (b) Distribution of equivalent elastic strain

The previous results justify the possibility of simplifying the simulation model of the PLA limiter by considering the arm bars as rigid bodies since the maximum calculated stress, 22.604 MPa, is much lower than the yield strength of the aluminum and there is no significant elastic deformation in this region. The maximum equivalent elastic deformation in the structure is about 0,2% and it occurs in the PLA bushing, since this material has low mechanical strength, which is 1.368%, below the material's limit of 1.568% , and the maximum von Mises stress in these elements is 8.94 MPa, below the yield strength of PLA, at 45.16 MPa. Both deformation and maximum stress occur in the left bushing, as the center of mass of the orthosis is displaced to the left due to the left horizontal bar being larger and consequently heavier than the right one, and the total weight of the forearm and the mass of the object is applied to this center of mass, leading to a tendency of stress and deformation accumulation on this side. Considering both materials present in this model, it has a safety factor of 5.

FEA was also performed with the elbow flexion limitation system, and these parts were modeled considering the use of PLA. Thus, the limiter was added and set to limit the elbow flexion to 90° - the angle of greatest loading - due to the low stress observed in the previous structural analysis. The bars that compose the portion attached to the user's arm were modeled as rigid bodies, except for the vertical bar connected to the limiting mechanism, as shown in Figure 9a. The simulation revealed maximum stress at the contact point between the screw, fixed to the vertical bar of the orthosis that limits joint rotation, and the movable pin of the limiter. This region had von Mises stress values of 120.38 MPa in the screw and 11.83 MPa in the pin, as shown in Figure 9b. Both maximum stress values are below the yield strength for the 30MnVS6 steel used in the screw and the PLA material used in the limiter elements. The estimated safety coefficient for the limiter mechanism is 4.58, and for the limiting screw, it is 6.64.

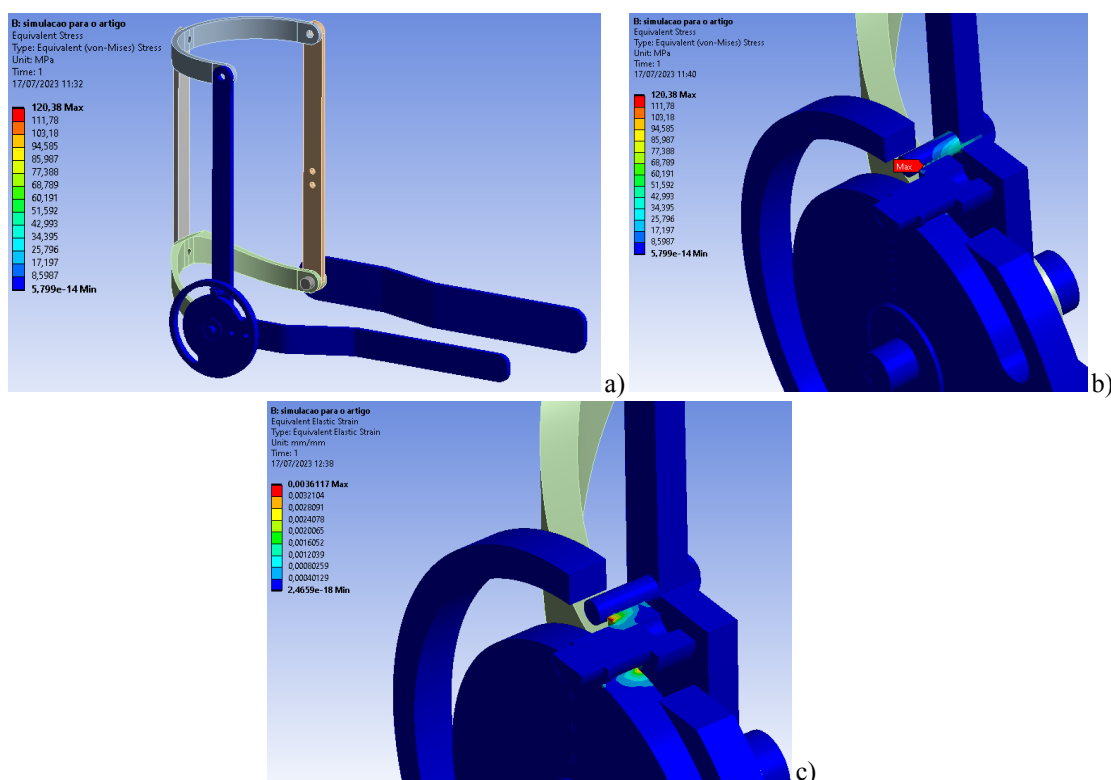


Figure 9. Results of the angular limiter simulation: (a) Distribution of von Mises stress on the structure of the orthosis (b) Distribution of von Mises stress on the angle limiter (c) Distribution of equivalent elastic strain

The average stress in the structure was 1.67MPa, below the values observed in the structural simulation, but such behavior can be explained by the accumulation of stress in the contact region of the angular limiter, where the maximum equivalent elastic deformation of 0.36%, as shown in Figure 9c, in addition to this region, it is noted that in the area of contact between the pin and the disc of the limiter, there is a region of deformation with values of 0.28%. Both equivalent elastic strains occur in PLA parts and are within the limits of maximum elastic strain.

4. CONCLUSION

This work focuses on the design of the orthosis for FES utilization, obtaining biomechanical data via software, and analyzing the mechanical structure for a static case. Inverse dynamics simulation was performed in Opensim software to obtain torques of 7 Nm and 4.62 Nm. The simulation results were corroborated by existing data in the literature, highlighting Opensim software as a powerful tool for obtaining biomechanical data in a practical, non-invasive, and cost-effective manner, as it is open-source software. For the analysis of the orthosis, two FEA simulations were conducted using ANSYS software. The obtained results indicate that the orthosis structure and the designed limiter are capable of withstanding the worst-case loading scenario. However, they also suggest the need for future work to equalize the left and right horizontal bars to reduce stress and deformation in the bushings, to perform a transient structural analysis to study the stress distribution in the orthosis, especially in the limiter, in case of muscle fatigue where the electrical stimulation is interrupted, and the limb undergoes sudden full extension, and to make a fatigue assessment because this movement will keep happen time to time and its necessary to know how the structure will behave.

5. ACKNOWLEDGMENTS

The authors would like to thank all members of LabBio for providing assistance and infrastructural support. We are also grateful for the partnership with the National Institute of Research in Digital Science and Technology (INRIA) in France. This work was funded by the Brazilian Agency for Industrial Research and Innovation (FINEP, agreement: 01.12.0476.00). We also acknowledge the support from the Minas Gerais Research Foundation (FAPEMIG) and this study was financed in part by the Coordenação de Aperfeiçoamento de Pessoal de Nível Superior - Brasil (CAPES) - Finance Code 001, grant (203345/2019-3).

6. REFERENCES

- ANSYS: Engineering Simulation Software. Version 2019R1. ANSYS, Inc., 2019.
- Donkor E.S. 2018. Stroke in the 21st Century: A Snapshot of the Burden, Epidemiology, and Quality of Life. *Stroke Res Treatment*. 2018 Nov 27;2018:3238165. doi: 10.1155/2018/3238165. PMID: 30598741; PMCID: PMC6288566.
- Ferreira, F.M.R.M., Rúbio, G.d.P., Dutra, R.M.A., Van Patten M.V.N., Vimieiro C.B.S., 2022. Development of portable robotic orthosis and biomechanical validation in people with limited upper limb function after stroke. *Robotica*, 40(12), 4238-4256. doi:10.1017/S0263574722000881
- IBGE. 2009. *Household Budget Survey 2008-2009: Analysis of Personal Food Consumption in Brazil / IBGE, Work Coordination and Income (in portuguese)*, Instituto Brasileiro de Geografia e Estatística, IBGE, Rio de Janeiro, <https://biblioteca.ibge.gov.br/visualizacao/livros/liv50063.pdf> . Accessed 7 March 2023.
- Lavrenko, I., Lebedysnskyi B., 2022. “Determination of the stress-strains state of the structural elements of the elbow orthosis prototype”. *International Science Journal of Engineering & Agriculture*. Vol. 1, No 3, 2022, pp. 29-36. doi: 10.46299/j.isjea.20220103.3.
- OPENSIM, 2010. *Opensim Documentation (web publications)*, 2010. Initial page. <<https://simtk-confluence.stanford.edu:8443/display/OpenSim/Documentation>>. Accessed 4 May 2023.
- Ovako, 2011. *MatWeb: material property data (web publications)*. <<https://www.matweb.com/search/DataSheet.aspx?MatGUID=e288d25c76e641b4acb26399576c5bb8&ckck=1>>. Accessed 12 June 2023.
- Seth A, Hicks JL, Uchida TK, Habib A, Dembia CL, Dunne JJ, et al., 2018. OpenSim: Simulating musculoskeletal dynamics and neuromuscular control to study human and animal movement. *PLoS Comput Biol* 14(7): e1006223. <https://doi.org/10.1371/journal.pcbi.1006223>
- Lawrence, E.S., Coshall, C., Dunas, R., Stewart, J., Rudd, A.G., Howard, R., Wolfe, C.D.A., 2001. Estimates of the prevalence of acute stroke impairments and disability in a multiethnic population. *Stroke*, v. 32, n. 6, p. 1279-1284, 2001.
- Methalgata, 2019. “*Technical table: Mechanical properties of laminated aluminum alloys (in portuguese)*.” <https://metalthaga.com.br/wp-content/uploads/2017/12/5-Propriedades-Mecanicas-Ligas-deAluminio-Laminadas.pdf>. Accessed 23 April 2023.
- Ministério da Saúde, 2019. “*Guide for prescription, concession, adaptation and maintenance of orthoses, protheses and media motion aid (in portuguese)*.” Brasília, Federal District, 2019. https://bvsm.s.saude.gov.br/bvs/publicacoes/guia_manutencao_orteses_proteses_auxiliares_locomocao.pdf Accessed 1 May 2023.
- Rúbio, G.d.P, Ferreira, F.M.R.M., Brandão, F.H.d.L., Machado, V.F., Tonelli, L.G., Kozan, R.F., Vimieiro C.B.S., 2019. “Design of actuators applied to an upper limb orthosis”. *In Proceedings of the 25th International Congress of Mechanical Engineering - COBEM 2019* , Uberlândia, MG, Brasil. doi: 10.26678/ABCM.COBEM2019.COB2019-0553.URL <http://www.sistema.abcm.org.br/articleFiles/download/25287>.
- Rúbio, G.d.P, Ferreira, F.M.R.M., Dutra, R.M.A., Mata, A.M., Bonfim, J.P.F., Vimieiro C.B.S., 2021. “Elbow module validation of a robotic orthosis for stroke rehabilitation.” *Stroke*, v. 32, n. 6, p. 1279-1284, 2001. *In Proceedings of the 26th International Mechanical Engineering-COBEM 2021*. Florianópolis, SC, Brasil. doi:
- World Health Organization, 2021. “World health statistics 2021: monitoring health for the SDGs, sustainable development goals.” World Health Organization. <https://apps.who.int/iris/handle/10665/342703>. License: CC BY-NC-SA 3.0 IGO

7. RESPONSIBILITY NOTICE

The authors are the only responsible for the printed material included in this paper.